AGU PUBLICATIONS

Geophysical Research Letters

RESEARCH LETTER
10.1002/2017GL073326

Key Points:
- Microscale pore network simulation verifies the experimentally observed electrical signature of ionic transport in dual-domain media
- The so-called bicontinuum model relating bulk and fluid conductivity in dual-domain media is not rigorously correct
- A new petrophysical model based on differential effective media theory is shown to reproduce experimental data and pore network simulations

Supporting Information:
- Supporting Information S1

Correspondence to:
F. D. Day-Lewis,
daylewis@usgs.gov

Citation:
Day-Lewis, F. D., N. Linde, R. Haggerty, K. Singha, and M. A. Briggs (2017), Pore network modeling of the electrical signature of solute transport in dual-domain media, *Geophys. Res. Lett.*, *44*, 4908–4916, doi:10.1002/2017GL073326.

Received 3 MAR 2017
Accepted 25 APR 2017
Accepted article online 27 APR 2017
Published online 29 MAY 2017

Pore network modeling of the electrical signature of solute transport in dual-domain media

F. D. Day-Lewis[1], N. Linde[2], R. Haggerty[3], K. Singha[4], and M. A. Briggs[1]

[1]Office of Groundwater, Branch of Geophysics, U.S. Geological Survey, Storrs, Connecticut, USA, [2]Applied and Environmental Geophysics Group, Institute of Earth Sciences, University of Lausanne, Lausanne, Switzerland, [3]Research Office, Oregon State University, Corvallis, Oregon, USA, [4]Hydrologic Sciences and Engineering Program, Geology and Geological Engineering Department, Colorado School of Mines, Golden, Colorado, USA

Abstract Dual-domain models are used to explain anomalous solute transport behavior observed in diverse hydrologic settings and applications, from groundwater remediation to hyporheic exchange. To constrain such models, new methods are needed with sensitivity to both immobile and mobile domains. Recent experiments indicate that dual-domain transport of ionic tracers has an observable geoelectrical signature, appearing as a nonlinear, hysteretic relation between paired bulk and fluid electrical conductivity. Here we present a mechanistic explanation for this geoelectrical signature and evaluate assumptions underlying a previously published petrophysical model for bulk conductivity in dual-domain media. Pore network modeling of fluid flow, solute transport, and electrical conduction (1) verifies the geoelectrical signature of dual-domain transport, (2) reveals limitations of the previously used petrophysical model, and (3) demonstrates that a new petrophysical model, based on differential effective media theory, closely approximates the simulated bulk/fluid conductivity relation. These findings underscore the potential of geophysically based calibration of dual-domain models.

Plain Language Summary In many geologic settings, the migration of chemicals in groundwater does not appear to obey the classical theory of advective-dispersive transport in porous materials. Instead, it is necessary to represent the rock or soil through which water moves as comprising two overlapping domains, one in which water and chemicals move (the mobile domain), and the other in which water is stagnant and chemicals are trapped for some period of time (the immobile domain). Such dual-domain models are used to reproduce tracer data and describe transport observations from contaminated sites, water-resource investigations, and aquifer management operations; however, estimating the parameters for dual-domain models is difficult because the immobile domain is inaccessible to conventional sampling. Electrical geophysical methods have been shown to be sensitive to the immobile domain and exchange between mobile and immobile domains. Previous experimental studies indicate that a time-varying, or hysteretic, relation can develop during transport of electrically conductive tracers through dual-domain materials. Here, we (1) provide a micro-scale mechanistic explanation for such observations and verify the electrical signature of transport in dual-domain materials, and (2) present a new petrophysical model to link electrical measurements and the electrical conductivity of pore fluids.

1. Introduction

In numerous field-scale studies of solute transport (i.e., tracer tests, contaminant migration, and aquifer storage recovery), concentration tailing and rebound behavior have been observed and modeled using dual porosity (also known as dual-domain or mobile/immobile) models [e.g., *Haggerty and Gorelick*, 1995; *Feehley and Zheng*, 2000]. In such models, the aquifer medium is conceptualized as consisting of overlapping continua, comprising (1) the well-connected pores and (or) transmissive fractures (i.e., the mobile domain), in which advection and dispersion occur, and (2) the poorly connected or otherwise flow-obstructed pores and (or) dead-end fractures (i.e., the immobile domain or less-mobile domain). Exchange between the domains is commonly represented by diffusion. Here for generality we use the multirate mass transfer (MRMT) formulation of *Haggerty and Gorelick* [1995], in which the immobile domain is divided into N compartments. In the absence of sorption, one-dimensional (1-D) transport is described by a system of $N + 1$ partial differential equations:

$$\theta_m \frac{\partial C_m}{\partial t} + \sum_{j=1}^{N} \theta_{im,j} \frac{\partial C_{im,j}}{\partial t} = \theta_m D \frac{\partial^2 C_m}{\partial x^2} - \theta_m \frac{\partial (C_m v)}{\partial x}, \text{and} \quad (1a)$$

$$\frac{\partial C_{im,j}}{\partial t} = \alpha_j (C_m - C_{im,j}), j = 1, \ldots, N, \quad (1b)$$

where α_j is the rate coefficient for immobile compartment j [/day], C_m is the mobile-domain concentration [M/L^3], $C_{im,j}$ is the concentration in compartment j associated with rate j [M/L^3], D is the molecular diffusion coefficient [L^2/T], v is the pore water velocity [L/T], θ_m is the mobile-domain porosity [−], $\theta_{im,j}$ is the porosity comprising immobile compartment j [−], and t is time [T]. MRMT allows for residence in the immobile domain to occur over a broad range of spatial and temporal scales. For a single-rate mass transfer (SRMT) formulation, equation (1b) reduces to one equation.

Inference of the parameters controlling mass transfer (i.e., α and θ_{im}) is difficult because conventional sampling draws fluid from the mobile domain and provides only indirect information about the concentration history in the upgradient immobile domain. Even with extensive coring, it is not possible to sample all scales of heterogeneity. New experimental approaches are required to infer mass transfer rate coefficients, immobile porosity, and immobile contaminant mass.

There is mounting laboratory and field experimental evidence that anomalous transport has an observable electrical signature during tracer experiments when fluid conductivities in the mobile and immobile domains differ [*Singha et al*., 2007; *Swanson et al*., 2012, 2015; *Briggs et al*., 2013, 2014]. Whereas conventional measurements are sensitive only to mobile concentration, electrical measurements are sensitive to both mobile and immobile concentration; thus, a time-varying or hysteretic relation between bulk and fluid conductivity during ionic tracer breakthrough can develop as a signature of anomalous transport. The combination of tracer tests and geophysical monitoring has potential to improve inference of dual-domain parameters [*Day-Lewis and Singha*, 2008; *Briggs et al*., 2013, 2014].

Singha et al. [2007] developed a so-called bicontinuum extension to Archie's law [*Archie*, 1942] assuming (1) that mobile and immobile domains are filled with water of electrical conductivity σ_m and σ_{im}, respectively, and behave as conductors in parallel, i.e., with volume-weighted arithmetic averaging, and (2) surface conduction is negligible:

$$\sigma_e = (\theta_m + \theta_{im})^{m-1} (\theta_m \sigma_m + \theta_{im} \sigma_{im}), \quad (2)$$

where σ_e is effective bulk conductivity [S/m] and m [−] is Archie's cementation exponent, which is a function of pore connectivity and tortuosity. (In our notation the subscript "m" indicates mobile, as in equations (1a) and (1b), whereas the cementation exponent, m, is a variable and thus italicized.) This petrophysical model has been used to qualitatively reproduce field data [*Singha et al*., 2007] and calibrate numerical and analytical models [*Briggs et al*., 2013, 2014], but other petrophysical formulations could potentially offer higher predictive capability. A large body of literature exists on conductivity averaging [e.g., *Lesmes and Friedman*, 2005; *Cosenza et al*., 2010], but to the best of our knowledge, conductivity averaging between mobile and immobile porosity for dual-domain media has not been investigated further than by *Singha et al.* [2007] nor has the electrical signature of anomalous transport been mechanistically demonstrated using microscale models.

2. Pore Network Modeling

We investigate the microscale geoelectrical signature of mass transfer using a pore network model (PNM) with a pipe lattice representation of the pore space. PNMs have been used extensively in studies of petrophysics [e.g., *Jin and Sharma*, 1991; *Bernabé*, 1995; *Bernabé and Revil*, 1995; *Suman and Knight*, 1997; *Friedman and Seaton*, 1998; *Bernabé et al*., 2011; *Moysey and Liu*, 2012], solute transport [e.g., *Dearcangelis et al*., 1986; *Bijeljic and Blunt*, 2007], and multiphase flow [e.g., *Blunt et al*., 2002]. Our approach to the electrical conduction problem is similar to those of many other studies going back to *Greenberg and Brace* [1969]. Solution of direct current electrical conduction and steady state single-phase flow in a PNM is trivial. Our present contribution is in linking flow, transport, and electrical conduction to investigate the geoelectrical signature of mass transfer during tracer breakthrough (i.e., nonequilibrium conditions). For the transport problem, we solve for temporal moments of concentration rather than for concentration itself [*Harvey and Gorelick*, 1995],

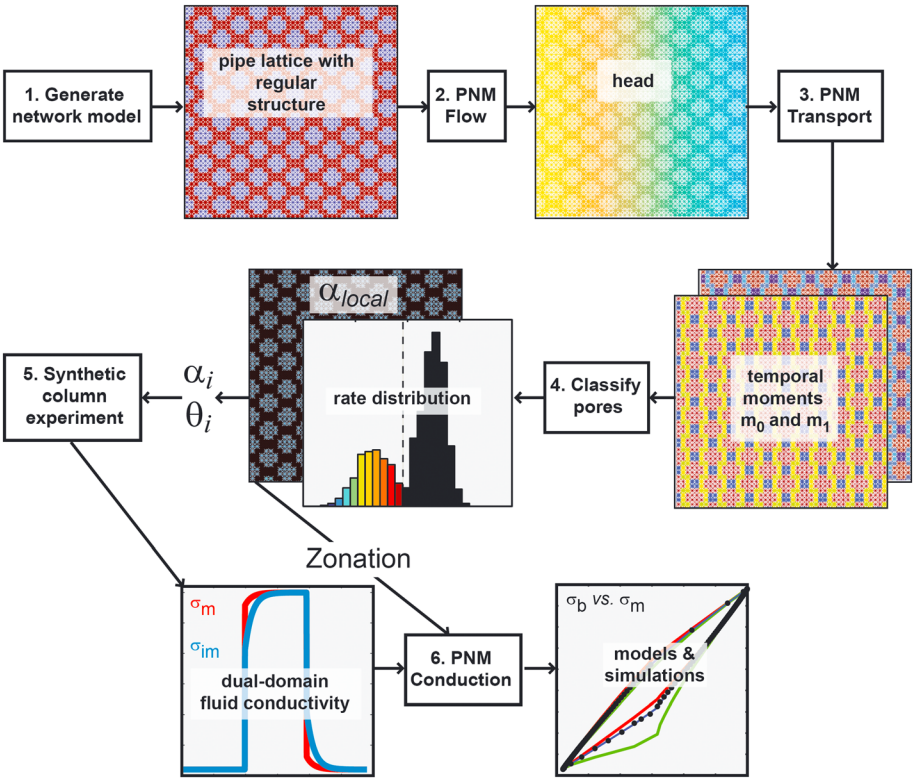

Figure 1. Schematic diagram illustrating our six-step pore network modeling approach to simulate the geoelectrical signature of solute transport through dual-domain geologic media.

thereby reducing computational requirements and providing direct insight into mass transfer. We note that more advanced and rigorous simulation approaches are found in the literature, for example, smoothed particle hydrodynamics [e.g., *Tartakovsky et al.*, 2007] and Lattice Boltzmann [e.g., *Kang et al.*, 2006]; however, a PNM is simple to implement and has immense computational advantage. In our work, transport simulations are required primarily to classify pores as mobile or immobile and to calculate pore residence times (or mass transfer rate coefficient, the reciprocal of residence time).

Our modeling approach includes six steps, illustrated schematically in Figure 1, summarized here, and explained in detail in the supporting information. Steps 1–5 follow the approach of *Briggs et al.* [2015], and the new step is merely the electrical conduction solution, which amounts to a resistor network problem. In Step 1, we generate a regular two-dimensional (2-D) pipe lattice (Figure 2). In Step 2, we solve the network flow problem for hydraulic head and calculate interpore flows according to the Hagen-Poiseuille Law. In Step 3, we solve a series of transport problems to calculate the advective-diffusive residence time for every pore and then assign pores to mobile or immobile domains based on a clustering algorithm. In Step 4, we solve a diffusive transport problem for each immobile region in the PNM to calculate the effective mass transfer rate coefficient associated with each region; these rate coefficients are taken as the distribution of α_i in equations (1a) and (1b). In Step 5, we solve equations (1a) and (1b) using a semianalytical model to simulate a column tracer experiment and produce mobile and immobile domain fluid conductivity time series, which are used to calculate electrical conductances. In Step 6, we solve the electrical problem and calculate bulk conductivity through time, thereby producing the relation between bulk conductivity and fluid conductivity in the mobile domain.

The pore network geometry (Figure 2) is designed to approximate the structure of the zeolite referred to as "Zeolite A" by *Swanson et al.* [2012, 2015] (Table 1). In the PNM, we represent intergranular and intragranular porosity as different classes of pores, class 1 and 2, respectively. Whereas each intergranular connection occurs through a single bond between adjacent pores, intragranular connections are divided between a number (N_B) of small bonds, consistent with CT scan visualizations of zeolite grains [*Swanson et al.*, 2012,

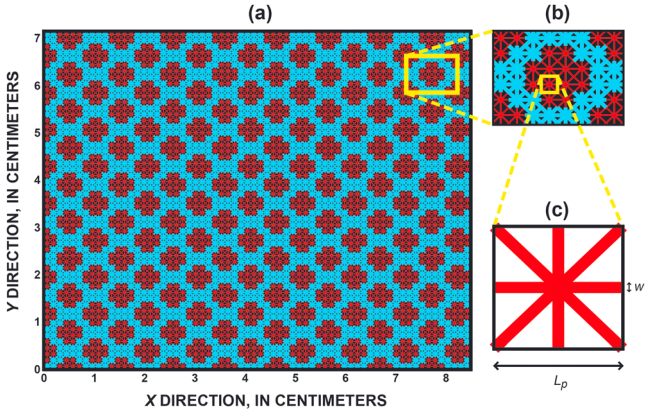

Figure 2. (a) Diagram showing the pore network model consisting of a pipe lattice; (b) enlarged view of pores representing a zeolite grain (red) surrounded by larger, open pores (blue); and (c) further enlarged view of a single pore internal to a zeolite grain.

2015]. Grains are represented as regions of class 2 pores with diameters based on the α_{SRMT} from *Briggs et al.* [2014] and the formula for the diffusive length scale of a spherical grain, $l_D = \sqrt{15D/\alpha} \approx 0.5$ cm [*Haggerty et al.*, 2000]. Each pore has a square cross section and is connected to its eight neighbors. The network comprises 66 pores (8.58 cm) in the *x* direction and 55 pores (7.15 cm) in the *y* direction. For simplicity, we assume uniform pore lengths, equal pore widths in the *x* and *y* directions, and a single layer in *z* with uniform pore thickness. Whereas the lattice geometry is designed to approximate the zeolite structure, the pore lengths, widths, and N_B were adjusted to achieve mobile and immobile porosities, mass transfer rate coefficients, hydraulic conductivity, and cementation exponent similar to that of the zeolite, as explained in section 4.

3. Laboratory Column Experiment

We consider data from a previously reported laboratory experiment [*Briggs et al.*, 2014] in which electrical measurements were collected during a NaCl tracer test in a column containing a granular zeolite (clinoptilolite). This zeolite was selected based on its high internal porosity (i.e., intragranular porosity), which constitutes the immobile pore space, making the material convenient for laboratory study of mass transfer although zeolite is not unique in exhibiting dual-domain behavior. Grain size ranges from about 2–4.8 mm. The maximum pore throat size associated with the immobile domain was estimated to be 30 μm [*Briggs et al.*, 2014] based on analysis of pressure cell data during elution tests using the technique of *Harvey* [1993]. Permeameter tests indicate a hydraulic conductivity of 0.5 cm/s.

In the *Briggs et al.* [2014] experiment, the PVC column was 0.4 m in length and 0.15 m in diameter (Figure 3a). Four electrodes in Wenner configuration were embedded within the column, arranged 0.025 m apart perpendicular to the column axis, at 25 cm from the inlet. Fluid electrical conductivity was monitored in the middle

Table 1. Pore Network Specifications and Properties of the Calibrated Network, With Calibration Targets Given in Parentheses

Network Specifications	
w, pore width (cm)	Class 1: 0.012; class 2: 0.032
N_B, # bonds	Class 1: 1; class 2: 12
L_p, pore length (cm)	0.13
Calibrated Network Properties	
θ, total porosity (−)	0.65 (0.63–0.65)
θ_m, mobile porosity (−)	0.45 (0.43–0.46)
θ_{im}, immobile porosity (−)	0.20 (0.17–0.22)
α_{SRMT}, rate coefficient (d^{-1})	112 (95–119)
m, cementation exponent (−)	2.35 (2.2)
K, hydraulic conductivity (cm/s)	0.57 (0.5)

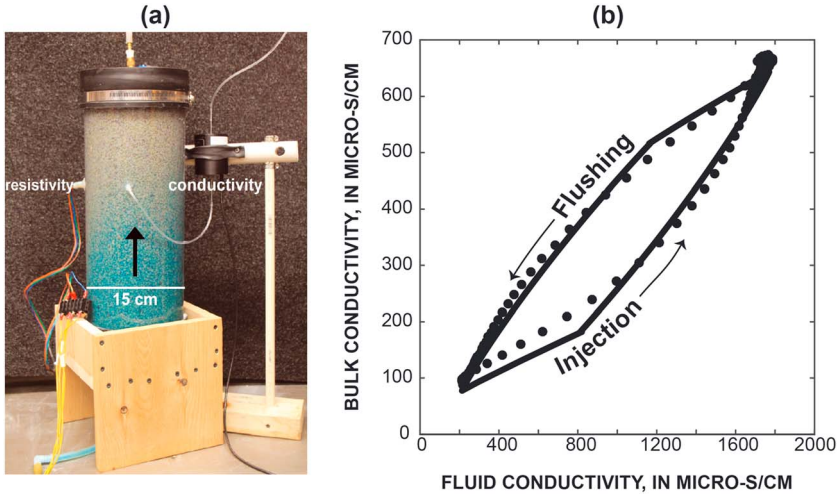

Figure 3. (a) Photograph of experimental setup and (b) bulk/fluid conductivity hysteresis loop from experiments in *Briggs et al.* [2014] (circles) and calibrated PNM simulation (solid line).

of the four electrodes. *Briggs et al.* [2014] subtracted the effect of measured surface conductivity (76 μS/cm), assumed to be constant throughout the experiment (Figure 3b). The cementation exponent was estimated to be 2.2 based on bulk and fluid measurements for three different equilibrium conductivity conditions. Following a period of flushing with tap water (approximately σ_f = 215 μS/cm at 20°C), a conductive NaCl tracer solution (σ_f = 1770 μS/cm) was injected at a constant rate for 22.1 h, after which the column was flushed again with tap water at the same injection rate for a total experiment duration of 29.2 h. The average linear pore fluid velocity in the *x* direction was estimated to be 13.9 m/d using the extracted fluid tracer breakthrough. *Briggs et al.* [2014] fit analytical and numerical models to the experimental data to estimate the parameters controlling single-rate mass transfer (SRMT) and found α_{SRMT} = 95 to 119 d^{-1}, θ_m = 0.43 to 0.46, and θ_{im} = 0.17 to 0.22. Note that α_{SRMT} is expressed here as inverse residence time rather than θ_{im} divided by residence time, as originally reported.

4. Pore Network Modeling Results

First, we calibrate the PNM to reproduce the experimental conditions and measurements of *Briggs et al.* [2014], presented in section 3. Second, we investigate averaging behavior between domains and compare results of the PNM simulations to petrophysical models for dual-domain media.

4.1. Model Construction and Calibration

Manual calibration of pore widths resulted in values of 120 μm for class 1 pores, and 320 μm for class 2 pores; these values produce adequate matches to the observed mobile porosity, immobile porosity, and hydraulic conductivity (Table 1). Manual calibration of the number of intragranular bonds to approximate the measured cementation exponent and hydraulic conductivity resulted in N_B = 12. The simulation results show hysteresis that is qualitatively similar to the laboratory data (Figure 3b). The bicontinuum model (equation (2)) of *Singha et al.* [2007] provides a poor approximation of the PNM results (Figure 4), overpredicting bulk conductivity during injection and underpredicting bulk conductivity during flushing. These results are not substantially improved by using the geometric or harmonic means in place of the arithmetic mean in equation (2), as further discussed in the supporting information. Indeed, the arithmetic and harmonic means appear not to bound the PNM results, contrary to effective media theory. We explain this apparent paradox subsequently.

4.2. Averaging Behavior

Inherent to the bicontinuum model of *Singha et al.* [2007] are the assumptions that a single formation factor in both domains can relate bulk and effective fluid conductivity and that the two fluid phases can be

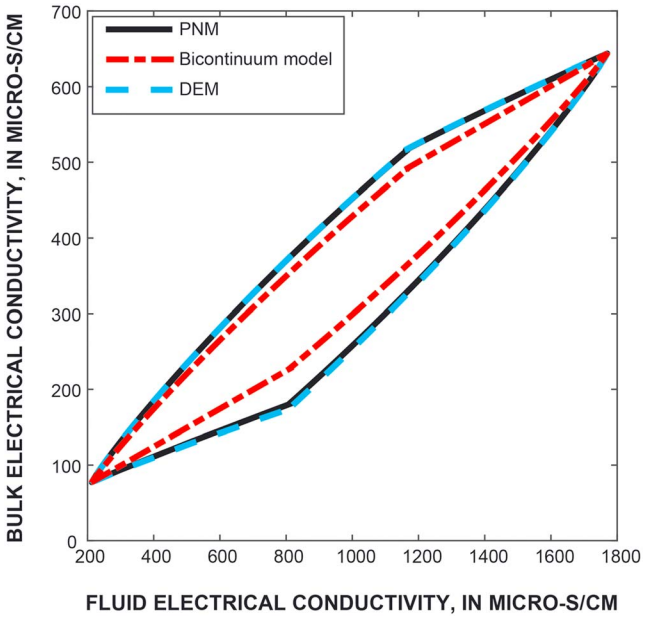

Figure 4. PNM simulation of the experimental hysteresis loop compared to petrophysical predictions based on the bicontinuum and DEM models of bulk conductivity.

averaged with weights based on porosity fractions, e.g., $\theta_m/(\theta_m + \theta_{im})$. The formation factor is defined (in the absence of surface conductivity) according to the formula commonly known as Archie's law:

$$\sigma_e = \theta^m \sigma_f = \frac{1}{F}\sigma_f, \tag{3}$$

where θ is total porosity, σ_f is fluid conductivity, and F is the formation factor. The assumption of a single formation factor for dual-domain media is not rigorously correct, as we now demonstrate. Consider a two-component system comprising parallel conductors with bulk conductivities σ_A and σ_B, square cross-sectional areas A_A and A_B, and identical length L. The effective conductivity for this simple system is given exactly by

$$\sigma_e = \frac{A_A\sigma_A/L + A_B\sigma_B/L}{A_A/L + A_B/L} = \frac{A_A\sigma_A + A_B\sigma_B}{A_A + A_B}, \tag{4}$$

showing that effective conductivity is a weighted arithmetic average of bulk conductivities. If the two conductors represent porous media with pore fluid conductivities of $\sigma_{f,A}$ and $\sigma_{f,B}$, and formation factors F_A and F_B, then according to Archie's law,

$$\sigma_e = \frac{\frac{1}{F_A}A_A\sigma_{f,A} + \frac{1}{F_B}A_B\sigma_{f,B}}{A_A + A_B}. \tag{5}$$

Although equation (5) shows that σ_e is a weighted arithmetic average of the fluid conductivities (as in equation (2)), the actual weights depend on the conductors' (1) cross-sectional areas, (2) internal porosities, and (3) internal pore space connectivity, as expressed by different formation factors or exponents; thus, the bulk conductivities predicted by Archie's law for each individual material are the appropriate quantities to be averaged, and the weights must consider bulk (not fluid) volume fractions. Assumption of a single, effective formation factor for both *A* and *B* may provide a poor approximation for the composite system if F_A and F_B differ strongly, such as in sediments with intragranular porosity; moreover, the porosity fraction weights in the bicontinuum model are not rigorously correct.

We propose, as an alternative to the bicontinuum model of *Singha et al.* [2007], a petrophysical model based on differential effective media (DEM) theory [*Sen et al.*, 1981; *Bussian*, 1983]. DEM theory provides a powerful framework to predict the effective properties of interacting mixtures. Whereas the bicontinuum model is developed by applying Archie's law to a weighted arithmetic average fluid conductivity for the two domains, we formulate the new model by applying DEM theory to average the two domains' bulk conductivities

calculated for each domain individually. The DEM model provides the effective bulk conductivity where the immobile domain bulk conductivity is embedded within the mobile domain bulk conductivity:

$$\sigma_e = \chi_1^n \left(\frac{\sigma_m}{F_1}\right)\left[\frac{1-\sigma_{im}F_1/(\sigma_m F_2)}{1-\sigma_{im}/(\sigma_e F_2)}\right]^n, \quad (6)$$

where $F_1 = \theta_1^{-m_1}$ and $F_2 = \theta_2^{-m_2}$ are formation factors for the intergranular (class 1) and intragranular (class 2) pores, respectively, θ_1 and θ_2 are the internal porosities of class 1 and class 2 pores, respectively, and χ_1 is the volume fraction of material 1 in the dual-porosity model; thus, χ_1 is the bulk volume of the class 1 regions divided by the total volume of the PNM, and $\theta_m = \chi_1\theta_1$ and $\theta_{im} = (1-\chi_1)\theta_2$. This self-consistent DEM model originates from multiple scattering theory [e.g., *Sen et al*., 1981] and treats the two domains symmetrically and allows for their interaction (i.e., no assumption of parallel conduction). The inconvenience of this generality is the model's implicit form, i.e., σ_e appears on the right-hand side of equation (6), which implies that a small iterative optimization problem must be solved.

There is a single value of the model parameter, n, for which Archie's law is obtained when the fluid conductivities are in equilibrium; thus, n is effectively constrained to

$$n = \frac{\log(F_1/F)}{\log\left(\chi_1 \frac{1-F_1/F_2}{1-F/F_2}\right)}, \quad (7)$$

where F is found by setting $\sigma_m = \sigma_{im}$ in the PNM and dividing assuming fluid conductivity by the calculated bulk conductivity. For the example considered here, n = 2.09. Compared to the bicontinuum model (equation (2)), the DEM model (equations (6) and (7)) provides a far superior match to the PNM simulation results (Figure 4). The relative mean absolute errors for the lower and upper limbs of the hysteresis curve are, respectively, 11.4% and 4.0% for the bicontinuum model, and 1.2% and 0.07% for the DEM model, where the errors are evaluated at 100 equally spaced points in terms of fluid conductivity.

5. Discussion

The DEM model (equations (6) and (7)) has strong theoretical underpinnings and performs extremely well, as expected given the consistency between DEM theory and the representation of zeolite grains as isolated inclusions; however, alternative models also could apply to dual-domain media, and there is extensive literature on effective properties [e.g., *Renard and de Marsily*, 1997]. In the supporting information, we consider the generalized power mean, which encompasses harmonic, geometric, and arithmetic averaging, as well as the two-phase models of *Pride* [1994] and *Glover et al.* [2000], which are functionally identical. Of the models considered, the DEM model provides the best match to the PNM results. Given that the mobile domain is expected to percolate by its very definition, immobile porosity will commonly comprise isolated regions, consistent with its representation in the DEM model.

Compared to the bicontinuum model of *Singha et al.* [2007], the DEM model requires additional information, i.e., the volume fractions and formation factors of the media constituting the dual domains. Additional work is required to incorporate the DEM model into the parameter inference approaches of *Briggs et al.* [2014] and to assess the applicability of the DEM and bicontinuum models to field data and different geologic media. In doing so, it will be necessary to account for the effect of surface conductivity (i.e., three conducting phases).

6. Conclusions

Dual-domain models of solute transport are used to understand and predict contaminant migration, groundwater remediation, and water resource management, yet information to calibrate such models is limited by the nature of dual-domain media, where the immobile domain is largely inaccessible to conventional field measurements. Previous work has shown the sensitivity of geoelectrical measurements to ionic tracer in the immobile domain [e.g., *Swanson et al*., 2012] and pointed to the potential of geophysical inference of dual-domain model parameters [e.g., *Briggs et al*., 2013, 2014], but those studies were limited by (1) lack of a mechanistic, microscale explanation for observations of a nonlinear, hysteretic relation between bulk and sampled fluid conductivity in contradiction to Archie's law; and (2) reliance on a petrophysical model that was based on the major assumption that the dual domains act as parallel conductors with a single formation factor. Here to overcome these limitations, we (1) developed a microscale PNM of flow, transport, and

electrical conduction, used the PNM to reproduce laboratory experimental data showing nonlinear hysteresis, and thus mechanistically explained the electrical signature of ionic transport in dual-domain media; and (2) presented a new petrophysical model for dual-domain media based on DEM theory and demonstrated that this model is more accurate than the model used in previous studies [*Singha et al*., 2007].

The PNM results support the conclusions of past experimental work that the hysteretic relation between bulk and fluid conductivity results from dual-domain exchange processes occurring local to the paired measurements and not along an upgradient flow path. Whereas analysis of conventional tracer experiments requires that the ratio of advection to exchange be close to 1 for inference of flow path-scale parameters, the use of electrical measurements can, in principle, allow for inference of highly localized parameters over a broad range of advective conditions. These developments provide a powerful new framework to understand and predict electrical averaging mechanics relevant to dual-domain media and support further application of emerging geophysical laboratory and field methodologies to study anomalous transport.

Acknowledgments
This work was supported by U.S. Department of Energy grant DE-SC0001773, the U.S. Geological Survey Toxic Substances Hydrology Program, U.S. Geological Survey Water Availability and Use Science Program, and National Science Foundation grants EAR-1446235 and EAR-1446300. The Herbette Foundation supported collaboration between the first and second authors. The experimental and model data are available in *Day-Lewis et al.* [2017].

References

Archie, G. E. (1942), The electrical resistivity log as an aid in determining some reservoir characteristics: Transactions of the American Institute of Mining, *Metall. Pet. Eng.*, *146*, 54–62.
Bernabé, Y. (1995), The transport properties of networks of cracks and pores, *J. Geophys. Res.*, *100*(B3), 4231–4241, doi:10.1029/94JB02986.
Bernabé, Y., and A. Revil (1995), Pore-scale heterogeneity, energy-dissipation and the transport properties of rocks, *Geophys. Res. Lett.*, *22*, 1529–1532.
Bernabé, Y., M. Zamora, M. Li, A. Maineult, and Y. B. Tang (2011), Pore connectivity, permeability, and electrical formation factor: A new model and comparison to experimental data, *J. Geophys. Res.*, *116*, B11204, doi:10.1029/2011JB008543.
Bijeljic, B., and M. J. Blunt (2007), Pore-scale modeling of transverse dispersion in porous media, *Water Resour. Res.*, *43*, W12S11, doi:10.1029/2006WR005700.
Blunt, M. J., M. D. Jackson, M. Piri, and P. H. Valvatne (2002), Detailed physics, predictive capabilities and macroscopic consequences for pore-network models of multiphase flow, *Adv. Water Resour.*, *25*, 1069–1089.
Briggs, M. A., F. D. Day-Lewis, G. P. Curtis, J. B. Ong, and J. W. Lane Jr. (2013), Simultaneous estimation of local-scale and flow path-scale dual-domain mass transfer parameters using geoelectrical monitoring, *Water Resour. Res.*, *49*, 5615–5630, doi:10.1002/wrcr.20397.
Briggs, M. A., F. D. Day-Lewis, J. B. Ong, J. W. Harvey, and J. W. Lane Jr. (2014), Dual-domain mass-transfer parameters from electrical hysteresis: Theory and analytical approach applied to laboratory, synthetic streambed, and groundwater experiments, *Water Resour. Res.*, *50*, 8281–8299, doi:10.1002/2014WR015880.
Briggs, M. A., F. D. Day-Lewis, J. P. Zarnetske, and J. W. Harvey (2015), A physical explanation for the development of redox microzones in hyporheic flow, *Geophys. Res. Lett.*, *42*, 4402–4410, doi:10.1002/2015GL064200.
Bussian, A. E. (1983), Electrical conductance in a porous medium, *Geophysics*, *49*, 1258–1268.
Cosenza, P., A. Ghorbani, C. Camerlynck, F. Rejiba, R. Guerin, and A. Tabbagh (2010), Effective medium theories for modeling the relationships between electromagnetic properties and hydrological variables in geomaterials: A review, *Near Surf. Geophys.*, *7*, 563–578.
Day-Lewis, F. D., and K. Singha (2008), Geoelectrical inference of mass transfer parameters: Theoretical basis and numerical experiments, *Water Resour. Res.*, *44*, W05201, doi:10.1029/2007WR006750.
Day-Lewis, F. D., N. Linde, R. Haggerty, K. Singha, and M. A. Briggs (2017), Model data for pore network modeling of the electrical signature of solute transport in dual-domain media, U.S. Geological Survey data release, doi:10.5066/F79C6VNB.
Dearcangelis, L., J. Koplik, S. Redner, and D. Wilkinson (1986), Hydrodynamic dispersion in network models of porous media, *Phys. Rev. Lett.*, *57*(8), 996–999.
Feehley, C. E., C. Zheng, and F. J. Molz (2000), A dual-domain mass transfer approach for modeling solute transport in heterogeneous porous media, application to the MADE site, *Water Resour. Res.*, *36*, 2501.
Friedman, S. P., and N. A. Seaton (1998), Critical path analysis of the relationship between permeability and electrical conductivity of three-dimensional pore networks, *Water Resour. Res.*, *34*(7), 1703–1710, doi:10.1029/98WR00939.
Glover, P. W. J., M. J. Hole, and J. Pous (2000), A modified Archie's law for two conducting phases, *Earth Planet. Sci. Lett.*, *180*, 369–383.
Goltz, M. N., and P. V. Roberts (1987), Using the method of moments to analyze three-dimensional diffusion-limited solute transport from temporal and spatial perspectives, *Water Resour. Res.*, *23*, 1575–1158.
Greenberg, R. J., and W. F. Brace (1969), Archie's law for rocks modeled by simple networks, *J. Geophys. Res.*, *74*, 2099–2102.
Haggerty, R., and S. M. Gorelick (1995), Multiple-rate mass transfer for modeling diffusion and surface reactions in media with pore-scale heterogeneity, *Water Resour. Res.*, *31*, 2383–2400.
Haggerty, R., S. A. McKenna, and L. Meigs (2000), On the late-time behavior of tracer test breakthrough curves, *Water Resour. Res.*, *36*, 3467–3347.
Harvey, J. W. (1993), Measurement of variation in soil solute tracer concentration across a range of effective pore sizes, *Water Resour. Res.*, *29*, 1831–1837.
Harvey, C. F., and S. M. Gorelick (1995), Temporal moment-generating equations: Modeling transport and mass transfer in heterogeneous aquifers, *Water Resour. Res.*, *31*, 1895–1911.
Hollenbeck, K. J. (1998), INVLAP.M: A matlab function for numerical inversion of Laplace transforms by the de Hoog algorithm, http://www.isva.dtu.dk/staff/karl/invlap.htm.
Jin, M., and M. Sharma (1991), A model for electrochemical and electrokinetic coupling in inhomogeneous porous media, *J. Colloid Interface Sci.*, *142*(1), 61–73.
Kang, Q., P. C. Lichtner, and D. Zhang (2006), Lattice Boltzmann pore-scale model for multicomponent reactive transport in porous media, *J. Geophys. Res.*, *111*, B05203, doi:10.1029/2005JB003951.
Leroy, P., and A. Revil (2004), A triple-layer model of the surface electrochemical properties of clay minerals, *J. Colloid Interface Sci.*, *270*, 371–380.
Lesmes, D. P., and S. P. Friedman (2005), Relationships between the electrical and hydrogeological properties of rocks and soils, in *Hydrogeophysics*, edited by Y. Rubin and S. S. Hubbard, pp. 87–128, Springer, Dordrecht, Netherlands.

Moysey, S. M., and Z. Liu (2012), Can the onset of macropore flow be detected using electrical resistivity measurements? *Soil Sci. Am. J.*, *76*(1), 10–17.

Pride, S. (1994), Governing equations for the coupled electromagnetics and acoustics of porous media, *Phys. Rev. B*, *50*, 15,678–15,696.

Renard, P., and G. de Marsily (1997), Calculating equivalent permeability: A review, *Adv. Water Resour.*, *20*(5–6), 253–278.

Revil, A., and M. Skold (2011), Salinity dependence of spectral induced polarization in sands and sandstones, *Geophys. J. Int.*, *187*, 813–824.

Revil, A., P. A. Pezard, and P. W. J. Glover (1999), Streaming potential in porous media. 1. Theory of the zeta potential, *J. Geophys. Res.*, *104*, 20,021–20,031.

Sen, P. N., C. Scale, and M. H. Cohen (1981), A self-similar model for sedimentary rocks with application to fused glass beads, *Geophysics*, *46*, 781–795.

Singha, K., F. D. Day-Lewis, and J. W. Lane Jr. (2007), Geoelectrical evidence of bicontinuum transport in groundwater, *Geophys. Res. Lett.*, *34*, L12401, doi:10.1029/2007GL030019.

Suman, R., and R. J. Knight (1997), Effects of pore structure and wettability on the electrical resistivity of partially saturated rocks—A network study, *Geophysics*, *62*, 1151–1162.

Swanson, R. D., K. Singha, F. D. Day-Lewis, A. Binley, K. Keating, and R. Haggerty (2012), Direct geoelectrical evidence of mass transfer at the laboratory scale, *Water Resour. Res.*, *48*, W10543, doi:10.1029/2012WR012431.

Swanson, R. D., A. Binley, K. Keating, S. France, G. Osterman, F. D. Day-Lewis, and K. Singha (2015), Anomalous solute transport in saturated porous media: Relating transport model parameters to electrical and nuclear magnetic resonance properties, *Water Resour. Res.*, *51*, 1264–1283, doi:10.1002/2014WR015284.

Tartakovsky, A. M., P. Meakin, T. D. Scheibe, and B. D. Wood (2007), A smoothed particle hydrodynamics model for reactive transport and mineral precipitation in porous and fractured porous media, *Water Resour. Res. 43*, W05437, doi:10.1029/2005WR004770.